19

STATE RESEARCH CENTER OF RUSSIA
Institute of Theoretical
and Experimental Physics

ITEP-24 -96

FERMILAB
AUG 21 1996
LIBRARY

M.Titov

ITEP-24-96

Muon Identification and Background studies at the HERA-B Experiment

NAME | I D No. | M.S.

Fermilab Library
0 1160 0066565 7

M o s c o w 1996

UDK 539.1 M-16

MUON IDENTIFICATION AND BACKGROUND STUDIES AT THE HERA-B EXPERIMENT:
Preprint ITEP 24-96/

M.Titov - M., 1996 - 20p.

В работе подробно исследуются источники ложной идентификации мюонов в эксперименте HERA-B и методы их подавления. Вероятность непосредственной идентификации адрона как мюона не превышает 1% во всем импульсном интервале. Предложенный метод поиска изломов на треках позволяет уменьшить фон от распадов на лету K и π мезонов соответственно в 10 и 3 раза. С учетом импульсных спектров оценка полной вероятности ложной идентификации адрона как мюона приводит к значениям $\approx 6 \cdot 10^{-3}$ для каонов и $\approx 8 \cdot 10^{-3}$ для пионов при сохранении высокой эффективности (99%) идентификации мюонов.

Fig. - 18, ref. - 6.

© Институт теоретической и экспериментальной физики, 1996

1 Introduction

HERA-B is an experiment dedicated to CP violation measurement, and also covering a wide range of other physics, which promises to be of high scientific value for the foreseeable future. Neutral B mesons provide one of the systems in nature, where CP violation phenomena might be observable. Unlike the kaon system, some B decay modes are predicted to show large CP asymmetries. In particular the decay $B \rightarrow J/\psi K_S^0 \rightarrow \ell^+\ell^-\pi^+\pi^-$ was accepted as the best candidate to study CP asymmetry. While the reconstruction of $J/\psi \rightarrow e^+e^-$ decay meets some problems [1], the $J/\psi \rightarrow \mu^+\mu^-$ decay channel appears to be very clean. Therefore, unambiguous muon identification plays a key role for the CP violation studies as well as for other important topics of the physics program announced.

The layout of the HERA-B spectrometer is shown in Fig.1.

A Silicon Vertex Detector (SVD) system measures tracks at the first 2 m of the HERA-B detector. The location of the magnet, with its center at 4.5 m downstream from the target, is a compromise between the acceptance for late-decaying K_s^0 - those decaying after the magnet are lost - and the magnet aperture for fixed solid angle coverage. In the region from $z \sim 2\ m$ (end of the SVD) to $z \sim 13\ m$, 15 (9 in the magnet) superlayers of the tracker chambers measure charge particle tracks, in almost the whole geometrical acceptance of the experiment. The ring imaging Cherenkov counter (RICH) placed at $z \sim 10\ m$ serves to identify kaons with momenta from a few GeV/c to 80 GeV/c. The transition radiation detector (TRD) followed by the electromagnetic calorimeter (ECAL) make up the electron identification system. Muon system identifies muon candidates as the tracks found in the tracker associated with the hits in the four superlayers of muon chambers, located at different depths in the absorber.

The separation of muons from hadrons is achieved exploiting higher penetration capability of muons. The total thickness of the absorber should be sufficient to reduce hadron punch-through to a level lower than the background rate due to pion and kaon decays-in-flight in SVD and in tracker. At the same time unambiguous matching of the track in the muon system to its trajectory in the tracker, where precise p and p_t determination is made, should be provided. As a compromise between these requirements, a 3 m thick absorber is used. This results in a low momentum cut-off of about 4.5 GeV/c.

Muon identification system of HERA-B is designed to

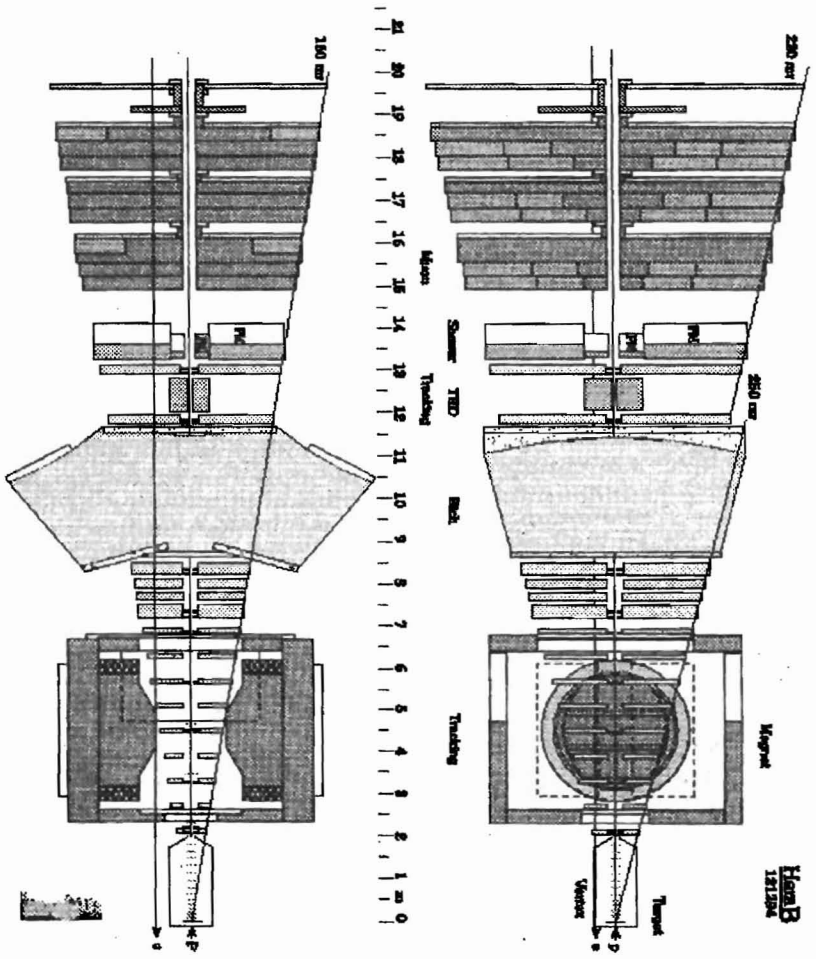

Figure 1: *The layout of the HERA-B detector*

- reconstruct muons from the decay $B \to J/\psi K_S^0$ followed by $J/\psi \to \mu\mu$;
- tag the initial flavour of b quark using charge of the muon originating from the decay of another b ;
- reconstruct the semileptonic decays of heavy quarks, and decays into lepton pairs.

Muon identification tools, background sources analysis and methods of background suppression are discussed below. Information from the muon system, tracker, RICH, ECAL and TRD can be used for identification of muon candidates.

2 Requirements for Muon Identification

Tagging of the b flavour is a crucial element of CP violation study. Studies of flavour non-specific states require to distinguish particles originating from B^0 meson and those originating from $\overline{B^0}$ meson. Tagging of the flavour by a full or even partial reconstruction of b-hadron would be inefficient due to small branching ratios and low reconstruction efficiencies. Instead, one can rely on the correlation between the charge of the muon and the flavour of the parent b-hadron. This results in a larger tagging efficiency, but sometimes leads to wrong tags.

When evaluating mistagging, several main effects have to be considered:

1) oscillations of B_d and B_s mesons results in wrong tags;

2) detected muon can be produced by the semileptonic charm decay in the $b \to c \to s(\mu)$ cascade, thus giving wrong tag;

3) muon can come from π or K decays-in-flight;

4) μ-hadron misidentification due to the hadronic punch-through.

The above sources of mistagging will reduce the observable CP asymmetry by a dilution factor D [1]. Since the error in $\sin(2\beta)$ is inversely proportional to $D\sqrt{\varepsilon}$, one defines [1] statistical power P of the tag:

$$P = D\sqrt{\varepsilon} = \frac{\varepsilon_{correct} - \varepsilon_{wrong}}{\sqrt{\varepsilon_{correct} + \varepsilon_{wrong} + \eta_{fake} \cdot N_b + \alpha \cdot \eta_{fake} \cdot N_{min.bias}}}$$

where ε - probability to find tag (with $p > 5\,GeV/c$, $p_t > 0.5\,GeV/c$) in the event with reconstructed $B \to J/\psi K_S^0$ decay; $\varepsilon_{correct} \simeq 0.051$ ($\varepsilon_{wrong} \simeq 0.013$) - probability to find correct (wrong) muon tag in the event with $B \to J/\psi K_S^0$ decay; η_{fake} is a muon fake rate; $N_b \simeq 0.15$ - mean number of pions and

kaons from decays of B-hadron per event; $N_{min.bias} \simeq 1.35$ - mean number of hadrons from minimum bias interactions per event; α - reduction factor for hadrons from minimum bias interactions due to the vertex cuts [1] (these and further results have been obtained using PYTHIA 5.6 and FRITIOF 7.0 event generators).

Fig. 2 shows the relative statistical power P of the muon tag as a function of muon fake rate η_{fake} for different values of α. $P(\eta_{fake}=0)$ is used for normalization.

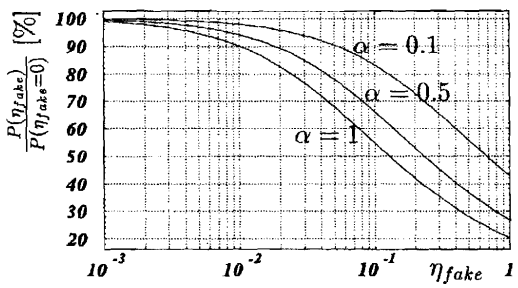

Figure 2: *The relative statistical power P of the muon tag as a function of muon fake rate for 3 different values of vertex reduction factor α. $P(\eta_{fake}=0)$ is used for normalization.*

The tagging power P falls with the increasing of the muon fake rate and substantially depends on the vertex reduction factor α for hadrons from minimum bias interactions. The relative statistical power P decreases on 10% at $\eta_{fake} = 10^{-2}$, without vertex cuts for tag candidates (α=1). If vertex suppression of the background is equal to 10 (α=0.1), the same decrease in P, 10%, is achieved at $\eta_{fake} = 5 \cdot 10^{-2}$. The most probable value of the reduction factor α is ranging between α=1 and α=0.1. It results in an admissible value of the muon fake rate of 1% - 5% for tag sample.

The straightforward estimation of the background rate for the $B \to J/\psi K_S^0$ decay is complicated because many of the background sources have large cross sections, compared to the signal process. One can estimate a muon fake rate η_{fake} for the $B \to J/\psi K_S^0$ ($J/\psi \to \mu^+\mu^-$) channel, assuming other reduction factors (mass, vertex and momentum cuts) to be factorized analytically.

Background undernearth the $B \to J/\psi K_S^0$ signal arises primarily due to the genuine or fake dileptons in the J/ψ mass range. The main sources of such dimuons are fake muons (due to K/π μ misidentification and hadron punch-through) and genuine muons (from events with charm quark production).

Muons from direct J/ψ, pass First Level Trigger almost without losses, but the vertex cut suppresses this backround to a level of two orders of magnitude lower compared to the signal [1, 2].

To estimate the background undernearth the J/ψ signal one should compare the number of fake muon pairs and the number of genuine muon and fake muon pairs ($\eta^2_{fake} \cdot < N_{ff} > + \eta_{fake} \cdot < N_{fc} > \cdot \varepsilon_c$) with the number genuine muon pairs ($< N_{cc} > \cdot \varepsilon_c^2$); where, η_{fake} is a muon fake rate, ε_c - efficiency of genuine muon identification; $< N_{fc} >$ - mean number of hadron-muon pairs from minimum-bias interactions per event; $< N_{ff} >$ - mean number of hadron pairs from minimum-bias interactions per event; $< N_{cc} >$ - mean number of muon pairs from the $c\bar{c} \rightarrow s\bar{s}(\mu^+\mu^-)$ decay in the event.

Taking $\frac{<N_{cc}>}{<N_{ff}>} = 1.3 \cdot 10^{-4}$ and $\frac{<N_{fc}>}{<N_{ff}>} = 3.2 \cdot 10^{-3}$, one can conclude that fakes at $\eta_{fake} \leq 1\%$ do not dominate.

Therefore for both physics processes discussed above the design goal is to reduce the muon fake rate from all background sources by a factor of about 100 while maintaining the highest possible efficiency for muons from b quarks.

3 Background Analysis

The following sources of background contribute to the muon misidentification

1) muons from hadronic showers in the absorber and hadron leakage through the muon shielding (hadronic punch-through);

2) muons from π / K decays-in-flight in the region between the target and the beginning of the muon system (hadron decays into muons in the absorber of the muon system are assigned to hadronic punch-through);

3) accident coincidence between track in the tracker and hits in the muon system (including background in the hall due to neutrons and soft photons);

4) background from the proton beam and beam optics.

Major background for muon identification in HERA-B comes from the decays-in-flight $\pi/K \rightarrow \mu\nu$ and hadronic punch-through. Therefore muon fake rate is the sum of two independent contributions: 1) hadronic punch-through, 2) decay probability for hadron to decay into muon in the HERA-B detector convoluted with the probability to identify such decay as a muon.

3.1 Hadronic Punch-through

We define the integral hadronic punch-through probability as the number of particles having hits in all muon superlayers divided by the total number of

incoming hadrons into the muon system. At large depths penetrating particles in the shower are predominantly muons coming from pion and kaons decays in the shower. In HERA-B experiment, the dominant rate is due to hadron decays.

The estimated punch-through probability for the HERA-B muon system (for details see [2]) as a function of hadron momentum is illustrated by Fig.3. The results obtained by GEANT simulation are in a good agreement with the experimental results of RD5 Collaboration [3].

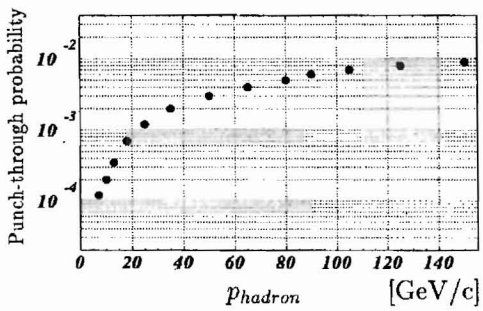

Figure 3: *Punch-through probability for the HERA-B muon system as a function of hadron momentum.*

To suppress background, muons from J/ψ (tag muons) required to have $p > 5\ GeV/c$ and $p_t > 0.5\ GeV/c$ ($p > 5\ GeV/c$ and $p_t > 1.0\ GeV/c$) as calculated in the magnet.

Fig.4 shows the number of fake muons due to the punch-through effect per event as a function of hadron momentum in the tracker. Taking into account the momentum spectrum of hadrons, we obtain the number $n_{fake}^{punch-through}$ of fake muons due to the punch-through effect per event:

$$n_{fake}^{punch-through} \simeq 1.0 \times 10^{-2} \qquad for \quad \mu(J/\psi) \quad candidates,$$

$$n_{fake}^{punch-through} \simeq 2.4 \times 10^{-3} \qquad for \quad \mu(tag) \quad candidates.$$

3.2 Hadron decays-in-flight

The signature of hadron decay-in-flight is a kink in the reconstructed track. Identification of such kinks is based on

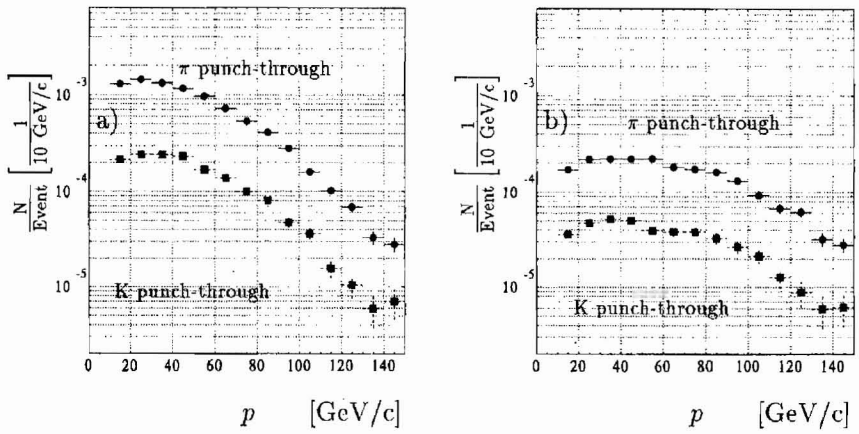

Figure 4: *Number of fake muons due to the hadron punch-through, per event as a function of particle momentum a) - for $\mu(J/\psi)$ candidates, b) - for $\mu(tag)$ candidates.*

- information from SVD and tracker in the region between the target and the first tracker superlayers;
- tracker information in the region of $3 < z < 10$ m;
- combined information from the last tracker superlayers and the muon system for $z > 10$ m.

To estimate the hadron-muon separation capability of the detector, the GEANT-based program was used. The results presented here were obtained using statistics of 10,000 events, each consisting of 5 minimum bias interactions.

3.2.1 Kinematics of muons from K/π decays

Fig. 5 shows the number of muons from π/K decays reaching the last tracker superlayer (open histogram) and the last muon superlayer (hatched histogram) as a function of z-coordinate of the decay point. The decays of secondary (and consequently soft) K and π lead to an increase in the number of muons from hadron decays-in-flight with z. Such π and K mainly originate from the regions of RICH and ECAL. The difference in open and hatched histograms is due to the loss of soft muons ($p < 4.5$ GeV/c) in the absorber of the muon system.

The simulation shows that the average reconstructed momentum of muons from π decay is $< p_\pi^\mu > \simeq 15\ GeV/c$ and from K decay $< p_K^\mu > \simeq 11\ GeV/c$, while the momentum of muons from B-decay is about 45 GeV/c. The cut at 5 GeV/c rejects the background considerably with the negligible loss in efficiency. The p and p_t distributions for the muons from $K/\pi \rightarrow \mu\nu$ are shown in fig.6.

The above requirements ($p > 5\ GeV/c, p_t > 0.5\ GeV/c$, and requirement of hits in all superlayers of the muon system (Fig.5,6)) eliminate 87% of muons from K meson (both primary and secondary) decays and 92% of muons from π meson (both primary and secondary) decays. Further analysis concerns only muons surviving these cuts.

3.2.2 Identification of the $K/\pi \rightarrow \mu\ \nu$ decays in tracker

In this section two possible criteria to identify kinks in tracker are discussed.

Global χ^2 method.

The global χ^2 method [4] based on the information from the 15 tracker superlayers is a straightforward procedure to reject kinks. The appearance of the kink could lead to a case, when track is splitted by the pattern recognition into two segments in tracker. Therefore χ^2 of the track fit shows an appreciable increase for such decays [1]. The cut value χ^2_{cut} was chosen to maintain the efficiency of J/ψ muons at the level of 99%. For all μ candidates $\chi^2 < \chi^2_{cut}$ was required.

The fraction of kinks from pions and kaons $\mathcal{P}_{kink}$, rejected by this cut, is shown in Fig.7,8 as a function of z (momentum spectra of K and π from minimum bias events were used) and p .

The total χ^2 cut becomes less powerful for hadrons decaying in the region near the first or the last tracker superlayers. Besides, pion decays are less frequently rejected by this cut due to a smaller energy release of the decay and therefore a smaller change in the direction of decay muon, relative to the decaying particle. The probability to identify a pion kink as a function of the decay point z has two maximums: at $z \sim 450\ cm$ in the magnetic field, where the technique is sensitive to the change both in the momentum and the direction of the track, and the second at $z \sim 800\ cm$ due to the higher density of tracker superlayers in this region.

One should mention that a significant part of such kinks can be rejected already at the level of pattern recognition and track reconstruction, based on

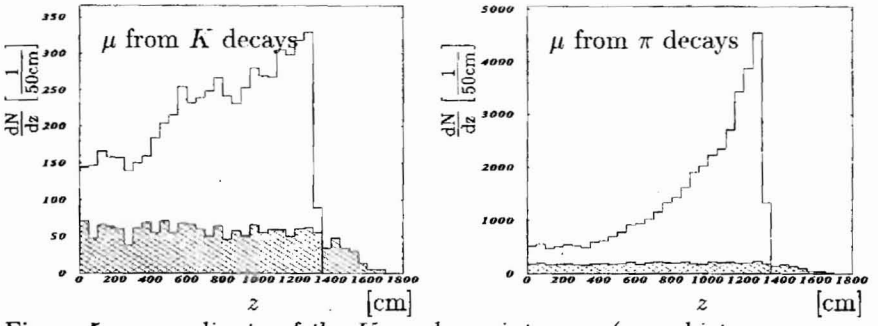

Figure 5: *z coordinate of the K, π decay into $\mu\nu$ (open histogram - muons from K/π decays reaching the last tracker superlayer, hatched histogram - muons from K/π decays reaching the last muon superlayer).*

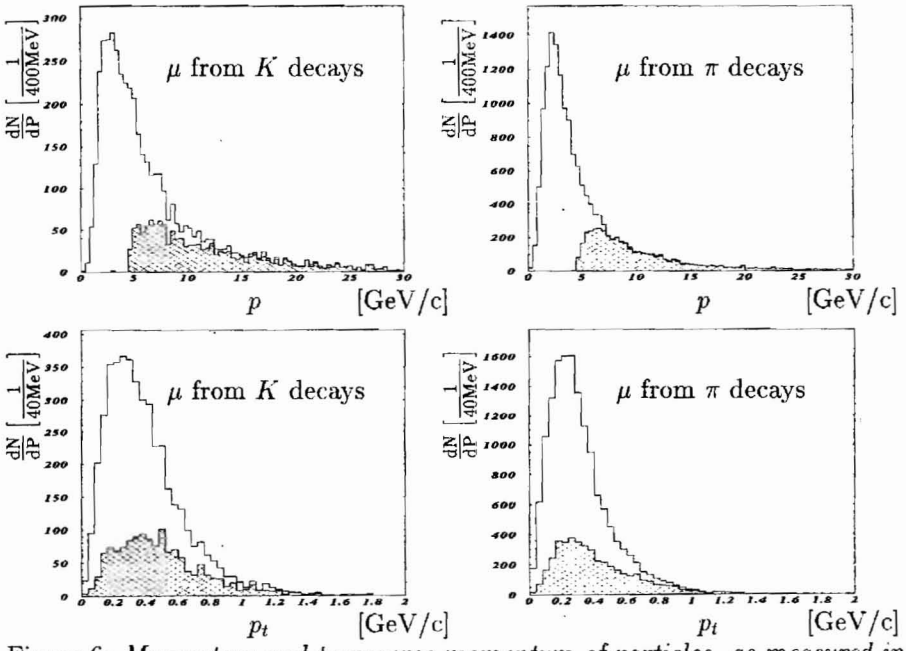

Figure 6: *Momentum and transverse momentum of particles as measured in magnet (open histogram - muons from K/π decays reaching the last tracker superlayer, hatched histogram - muons from K/π decays reaching the last muon superlayer).*

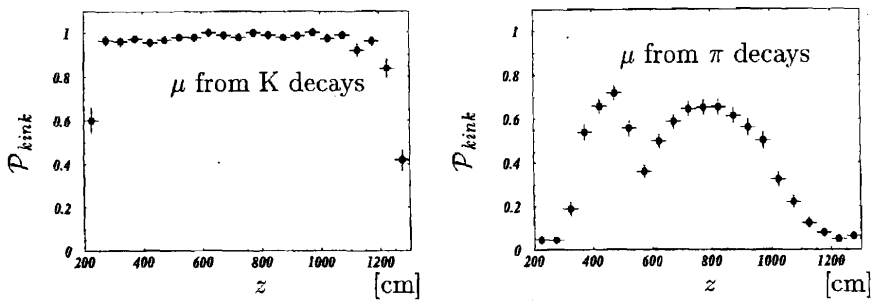

Figure 7: *The probability to identify kink by global χ^2 method as a function of the decay point.*

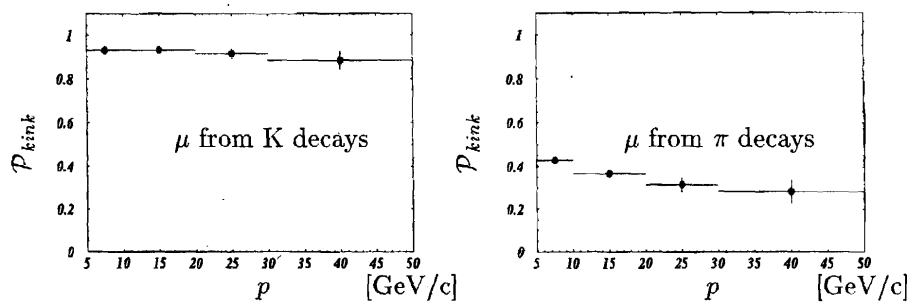

Figure 8: *The probability to identify kink by global χ^2 method as a function of a reconstructed pion and kaon momentum.*

the Kalman filter algorithm, that implies an upper cut on the increment of χ^2 calculating at each step.

Advanced χ^2 method.

Search for a kink in the interval between n and $n+1$ tracker superlayers is performed by fitting separately two track segments (one reconstructed from hits in $1..n$ superlayers, the other in $(n+1)..15$ superlayers), and merging them togerther. For both track segments their covariance matrices are computed for the track parameters in the point of merging (to simplify procedure every hit in the tracker is weighted with the function of distance from the merging point to hit according to multiple scattering). Then for any pair of a track segments with parameters $\vec{\alpha_i}$ (i= 1,2) and covariance matrices C_i , the χ^2 ansatz is written as

$$\chi^2 = (\vec{\alpha_1} - \vec{\alpha})^T \cdot C_1^{-1} \cdot (\vec{\alpha_1} - \vec{\alpha}) + (\vec{\alpha_2} - \vec{\alpha})^T \cdot C_2^{-1} \cdot (\vec{\alpha_2} - \vec{\alpha}),$$

where $\vec{\alpha}$ is the weighted mean

$$\vec{\alpha} = (C_1^{-1} + C_2^{-1}) \cdot (C_1^{-1} \cdot \vec{\alpha_1} + C_2^{-1} \cdot \vec{\alpha_2}).$$

This procedure gives 14 values of χ_n^2 ($n = 1..14$), corresponding to hypotheses of kink between each subsequent pair of 15 tracker superlayers. For any of the χ_n^2 values, the probability for the track under analysis to be a muon $P_\mu(\chi_n^2)$ we define as

$$P_\mu(\chi_n^2) = \frac{\int_{\chi_n^2}^{\infty} \rho_\mu(\chi^2)}{\int_0^{\infty} \rho_\mu(\chi^2)}$$

where $\rho_\mu(\chi^2)$ - the probability distribution of χ^2 for muons from J/ψ.

Then the probability of the kink within the interval n is

$$P_{kink}(\chi_n^2) = 1 - P_\mu(\chi_n^2).$$

Fig.9 illustrates the χ^2 values and associated probabilities $P_{kink}(\chi_n^2)$ of a kink to occur within each of the 14 intervals as obtained by this method. In the example chosen, π-meson with momentum $p \approx 10\ GeV/c$ decayed at $z = 607\ cm$. One of the advantages of this method is the by-product prediction of the most probable location of the decay point.

To estimate the rejection of muons from π/K decays, we propose to make use of the maximum sum $P^{sum}(\chi^2)$ of the decay probabilities $P_{kink}(\chi^2)$ in the 3 neighboring intervals. This makes use of sensitivity of the method not only in the interval containing kink, but also in the neighbouring intervals. The cut value $P_{cut}^{sum}(\chi^2)$ for J/ψ muons was chosen to maintain the efficiency at the same level, 99%, as in the first method. To assign track candidate to the decay-in-flight muon, $P^{sum}(\chi^2)$ should be greater than $P_{cut}^{sum}(\chi^2)$.

The probability $\mathcal{P}_{kink}$ of the π/K decay to be identified as a function of the momentum and z-coordinate of the decay point is shown in Fig.10,11.

3.2.3 Method application to B decays

Signal to background ratio optimization is one of the central questions in the physics analysis, where the efficiency and rejection interplay is important. Considering kink contribution to the background, one should take an advantage of relatively soft spectrum of kinks from decays-in-flight. The momentum spectrum of signal muons depends on the physics process considered. Therefore it is natural to use momentum dependent cuts, which requires the

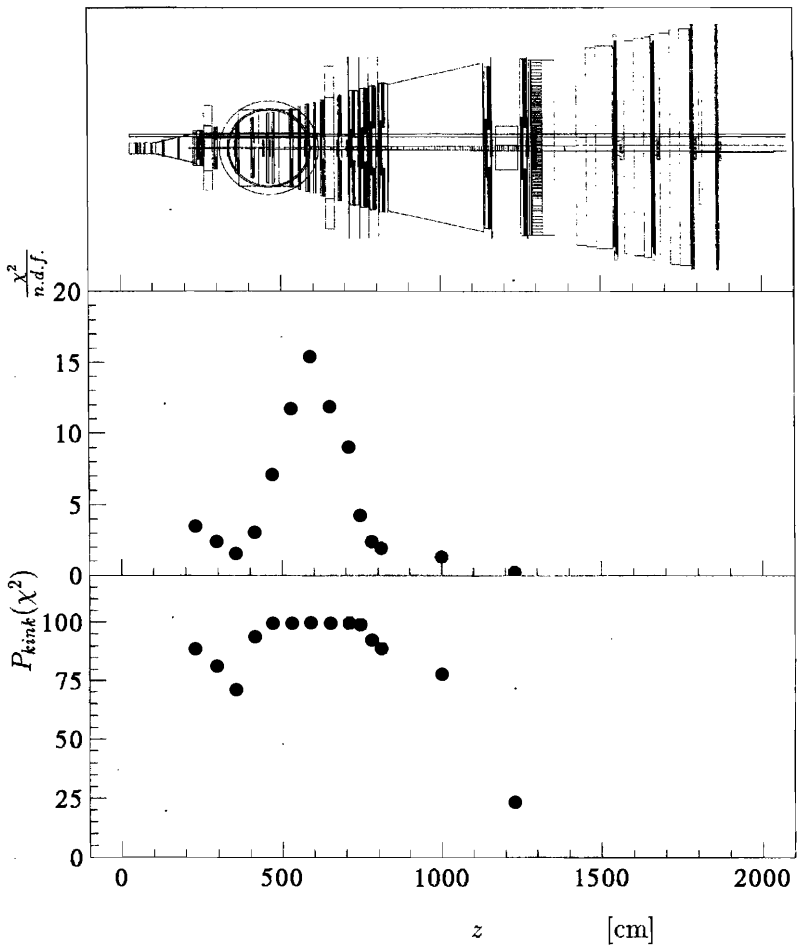

Figure 9: *The χ^2 distribution and associated probabilities $P_{kink}(\chi^2)$ for the kink to be found within each interval between subsequent tracker superlayers.*

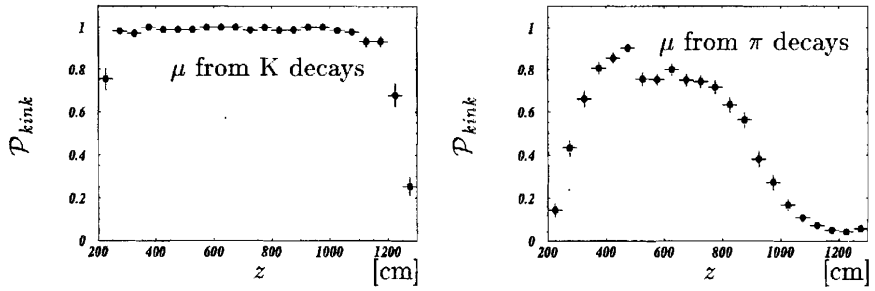

Figure 10: *The probability to identify kink by advanced χ^2 method as a function of the decay point.*

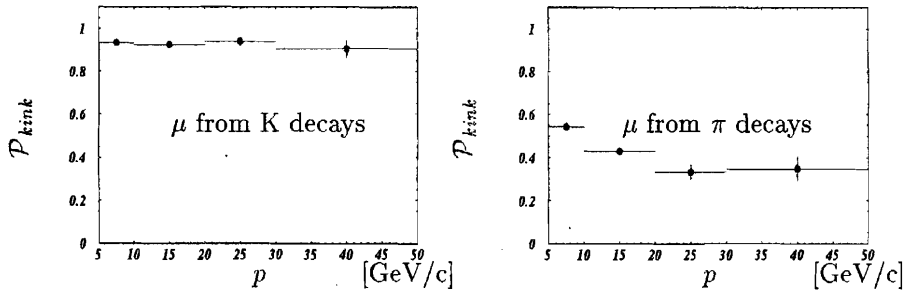

Figure 11: *The probability to identify kink by advanced χ^2 method as a function of the reconstructed kaon and pion momentum.*

study of muon efficiency ε_μ and rejection capability $\mathcal{P}$ of the method in all the momentum range.

The whole momentum spectrum was divided into 4 regions : 5 - 10 GeV/c, 10 - 20 GeV/c, 20 - 30 GeV/c and above 30 GeV/c. In each momentum interval the rejection of muons from $K/\pi \rightarrow \mu\nu$ decays was obtained for different muon efficiencies, ranging from $\varepsilon_\mu = 99\%$ to 90% (see Fig.12).

The momentum dependent cuts can be efficiently applied for muons from B decays. This is illustrated by Fig. 13,14 with the efficiency ε_μ of 90% chosen for $p =$ 5-10 GeV/c, 97% for $p =$ 10-20 GeV/c, 98% for $p =$ 20-30 GeV/c, 99.7% for momenta above 30 GeV/c, thus given the total efficiency $\varepsilon_\mu = 99\%$. Using these cuts we improve kink identification probability after SVD from $\sim$ 85% to $\sim$ 90% for kaons, and from $\sim$ 40% to $\sim$ 60% for pions. This leads to a rejection factor of about 10 for kaon and 2 to 3 for pion decays-in-flight. The muon fake rate η^{kink}_{fake} after cuts applied, is shown on Fig.15.

From the convolution of muon fake rate η^{kink}_{fake} and momentum spectrum of

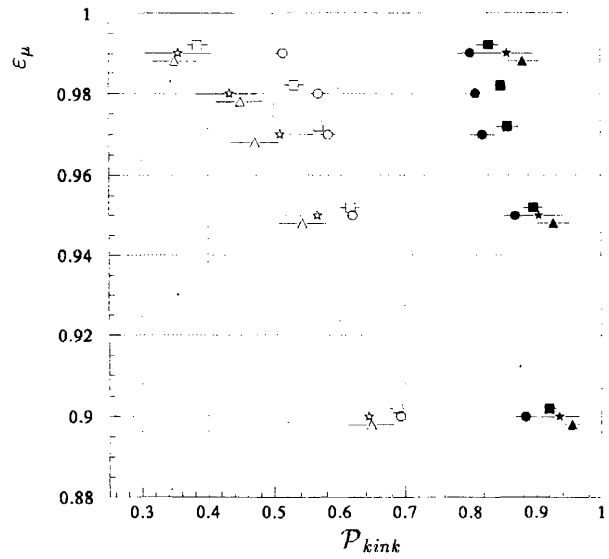

Figure 12: *The muon efficiency ε_μ as a function of kink rejection probability $\mathcal{P}_{kink}$ for different intervals of particle momentum (circles correspond to p = 5-10 GeV/c, squares to p = 10-20 GeV/c, triangles to p = 20-30 GeV/c, stars to momenta above 30 GeV/c. Open symbols represent muons from π decays, filled - muons from K decays.*

hadrons, we obtain the number n_{fake}^{kink} of fake muons due to the K/π decays-in-flight effect per event

$$n_{fake}^{kink} \simeq 4.3 \times 10^{-2} \qquad for \quad \mu(J/\psi) \quad candidates;$$

$$n_{fake}^{kink} \simeq 5.5 \times 10^{-3} \qquad for \quad \mu(tag) \quad candidates.$$

Combining these numbers with $n_{fake}^{punch-through}$ from hadronic punch-through we obtain the number of fake muons per event (see fig.17)

$$n_{fake} \simeq 5.3 \times 10^{-2} \qquad for \quad \mu(J/\psi) \quad candidates;$$

$$n_{fake} \simeq 7.9 \times 10^{-3} \qquad for \quad \mu(tag) \quad candidates.$$

The above analysis of the misidentification rate due to the decays-in-flight and punch-through provides a total μ-π misidentification probability of 0.8 % per pion. For μ-K misidentification the fake rate was found to be 0.6 % per kaon (see Fig.16)

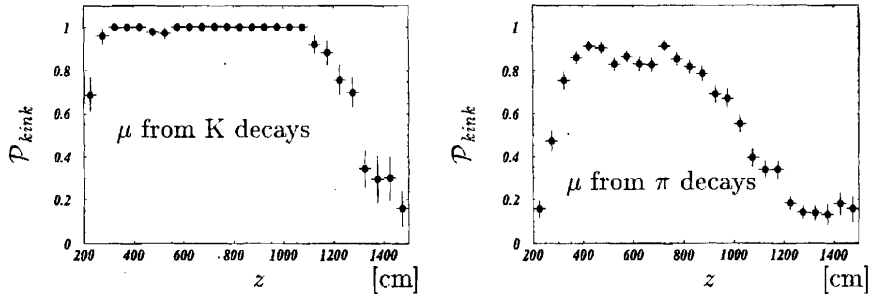

Figure 13: *The probability to identify kink by advanced χ^2 method as a function of the decay point.*

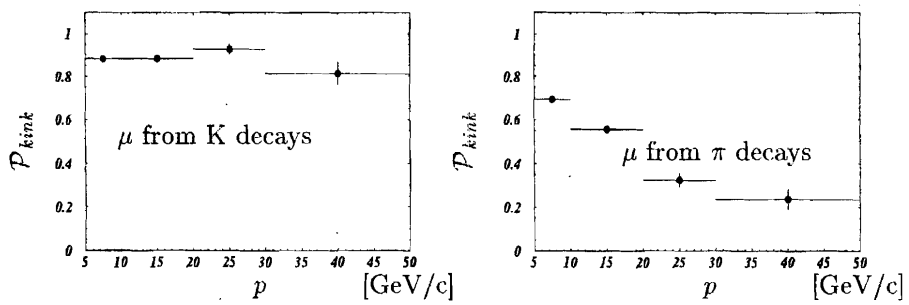

Figure 14: *The probability to identify kink by advanced χ^2 method as a function of the constructed kaon and pion momentum.*

It was assumed that the pattern recognititon and track reconstruction procedure in the SVD rejects 100% of kinks in the region $z < 2\ m$ due to the high intrinsic resolution. Moreover muons from decays-in-flight in the SVD region have an additional kinematic suppression due to the softer spectrum of secondary muons with respect to that of primary hadrons. The actual rejection of the decays-in-flight with the help of information from SVD should be studied relying on the given performance of SVD. The fake muons coming from the decays-in-flight in the region of SVD can be treated independently from the analysis above. The number of kinks in SVD having survived the rejection procedure, could be simply added to the number n_{fake} obtained. The SVD incorporation in the method described in this section also leads to an improvement of the rejection capabilities in the region of the first tracker superlayers.

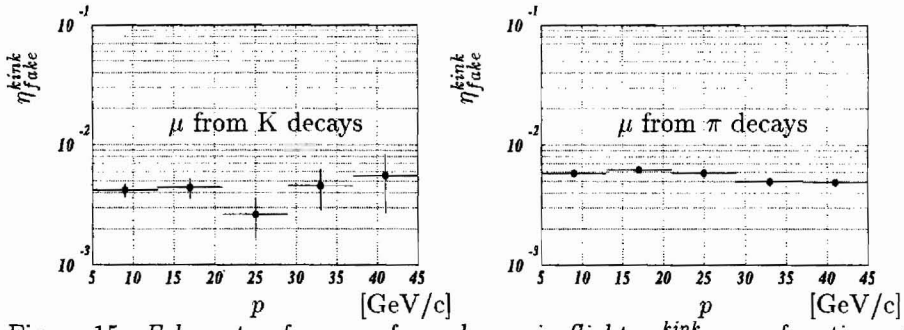

Figure 15: *Fake rate of muons from decays-in-flight* η_{fake}^{kink} *as a function of the reconstructed momentum.*

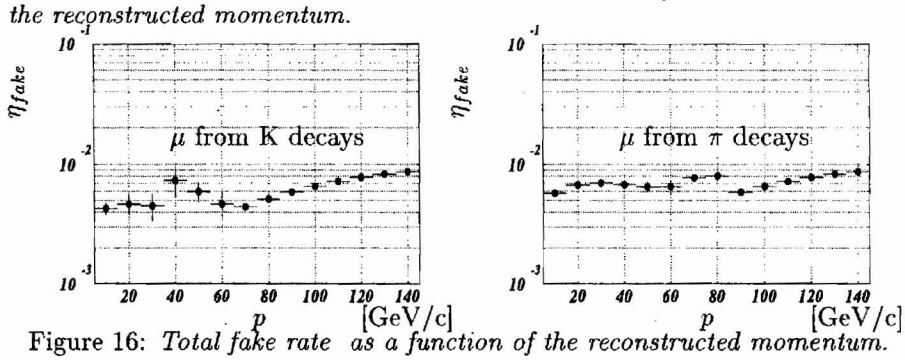

Figure 16: *Total fake rate as a function of the reconstructed momentum.*

4 Additional possibilities to improve muon identification

As discussed in Sec.3 a reliable identification of the decays-in-flight is achieved for the kinks in the region before RICH. At the same time only about 50 % of K $\rightarrow \mu\nu$ and 30 % $\pi \rightarrow \mu\nu$ decays (see Fig.10) in the region $z > 10\ m$ can be rejected. Therefore additional treatments are encouraged to suppress this background.

One of the most promising strategies employs the RICH counter information. RICH can efficiently improve the rejection of $K/\pi \rightarrow \mu\nu$ decays in the region after magnet. The muon coming from decay-in-flight in the region after magnet and before RICH produces ring with the radius inconsistent with the track momentum measured in magnet for a given mass hypothesis. The decays in the RICH lead to a smearing of the rings, which is an additional information for kink identification.

The most valuable help from RICH is expected for hadron decays-in-flight

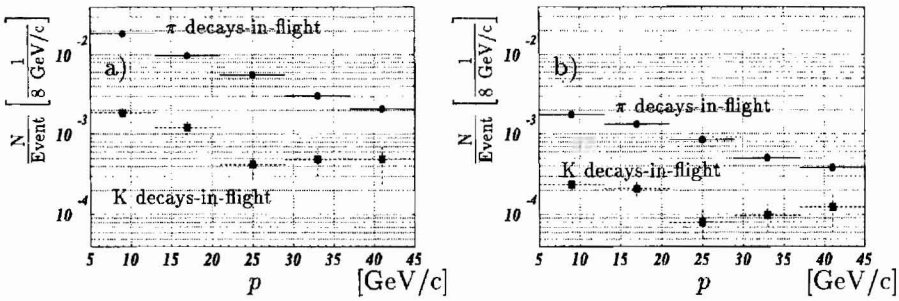

Figure 17: *Number of fake muons due to the K/π decays-in-flight per event as a function of particle momentum a) - for $\mu(J/\psi)$ candidates, b) - for $\mu(tag)$ candidates.*

after RICH and punch-through, since the χ^2 methods are less sensitive to the K/π decays in this region. μ and π masses are very close to each other compared to the K mass, therefore K-μ separation is of about the same quality as K-π separation (see Fig.18a, a detailed study of K-π separation is described in [1]). It is also possible to achieve a positive π-μ separation for pion momenta from 5 GeV/c to $\sim$ 15 GeV/c (see Fig.18b). Note, that 84 % of the decaying π mesons after RICH lie in this momentum region, and can be effectively suppressed. The probability of the identification falls down with the increase in particle momentum. Both Figures 18a and 18b are obtained for a fixed muon efficiency of 98%. The RICH counter can thus enable K-μ and π-μ separation in the momentum region where hadron decays-in-flight are dominant source of background.

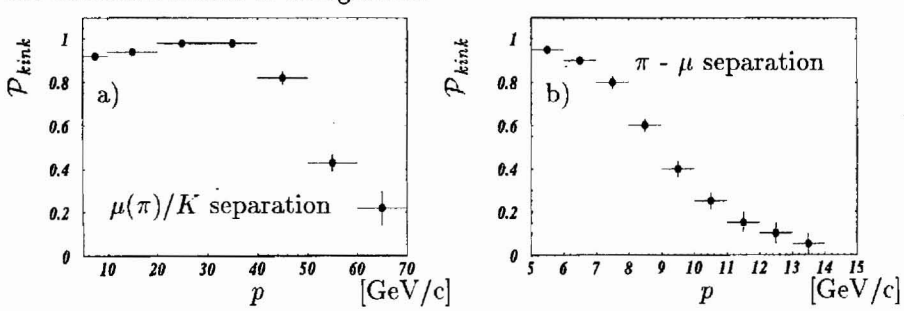

Figure 18: *Momentum dependence of the a) kaon b) pion separation for a fixed muon efficiency ε_μ=98%.*

The data from the ECAL could also contribute to the hadron-muon sep-

aration at HERA-B. The separation between hadrons and muons (the latter loose minimal energy compared to the particles hitting ECAL), substantially depends on the particle occupancy and hence from the distance to beam pipe. In the regions of low occupancy calorimeter could efficiently improve hadron-muon separation [5]. More sophisticated treatment including the detailed analysis of the shape and magnitude of energy deposition in ECAL, should be used in the regions of high occupancy.

Study of the muon identification with TRD was made in [6]. Good separation between muons and pions can be achieved for muon energies above 130 GeV/c. At this energies the dominant source of background is hadron punch-through, that can be additionally suppressed by TRD.

The information from RICH, ECAL and TRD can be included coherently with the one from tracker and muon system into global muon likelihood function.

5 Summary

The detailed analysis of background for muon identification in the HERA-B detector is presented.

The punch-through probability was found to be well below 1 % in the whole momentum region.

The method of kink identification based on advanced χ^2 technique, is developed using combined information from tracker and muon system. This method is more flexible compared to optimal fits handling big covariance matrices; contrary to conventional methods, the computation time is merely proportional to the number of track hits.

The proposed method of kink identification provides rejection at the level of 10 for kaon and 2 to 3 for pion decays-in-flight, that is particularily important for muons in the events with high hadron multiplicity. This results in the μ-K and μ-π misidentification fake rate of about $6 \cdot 10^{-3}$ per kaon and $8 \cdot 10^{-3}$ per pion respectively, while maintaining high reconstruction efficiency of about 99 % for muons.

Additional possibilities to improve muon identification with RICH, ECAL and TRD are proposed.

6 Acknowledgment

I am very grateful to M.Danilov and Yu.Zaitsev for useful and prolific discussions. It is a great pleasure to thank S.Barsuk, I.Belyaev, R.Kagan and S.Semenov for the most valuable help and stimulating discussions. I am thankful to all my colleagues from HERA-B Collaboration.

References

[1] T. Lohse *et al.*, HERA-B collaboration, An Experiment to Study CP Violation in the B System Using an Internal Target at the HERA Proton Ring, Proposal, **DESY-PRC 94/04** (1994).

[2] E. Hartouni *et al.*, HERA-B collaboration, An Experiment to Study CP Violation in the B System Using an Internal Target at the HERA Proton Ring, Design Report, **DESY-PRC 95/01** (1995).

[3] M.Aalste *et al.*, RD5 collaboration, Measurement of hadron shower punchthrough in iron, CERN-PPE/93-71, (1993)

[4] P.Billoir,R.Fruhwirth,M.Regler, Track element merging strategy and vertex fitting in complex modular detectors, Nucl.Instr. and Meth., **A241** (1985) 115-131.

[5] H.Albrecht *et al.*, ARGUS collaboration, Nucl.Instr. and Meth., **A275** (1989) 1-48.

[6] T.Akesson *et al.*, Particle identification performance of a straw Transition Radiation tracker prototype, CERN-PPE/95-111, (1995).